Available online at www.sciencedirect.com
SCIENCE DIRECT®
C. R. Chimie 8 (2005) 627–634
COMPTES RENDUS CHIMIE
http://france.elsevier.com/direct/CRAS2C/

Full paper / Mémoire

Hexagonal mesoporous silica nanoparticles with large pores and a hierarchical porosity tested for HPLC

Marco U. Martines [a,1], Erica Yeong [a,2], Michel Persin [a], André Larbot [a], W.F. Voorhout [b], C.K.U. Kübel [b], Patricia Kooyman [c], Eric Prouzet [a,*]

[a] *Institut Européen des Membranes (CNRS UMR 5635), CNRS, 1919 route de Mende, 34293 Montpellier cedex 5, France*
[b] *FEI Company, Application Laboratory, P.O. Box 80066, 5600KA Eindhoven, The Netherlands*
[c] *DCT/NBCHREM, Delft University of Technology, Julianalaan 136, 2628 BAL Delft, The Netherlands*

Received 14 June 2004; accepted after revision 18 October 2004

Available online 12 February 2005

Abstract

We report the preparation of a novel type of mesoporous silica of the MSU-type family. This material was prepared with Pluronic P123 copolymer in mild acidity according to a two-step process. Its structure was explored by X-ray diffraction, N2 isotherms, SEM and TEM. The TEM study was completed by a 3D tomography analysis that allowed us to obtain information on the morphology of the pore-and-void system. The powder is homogeneous and made of nanoparticles (200 nm in size) built by the folding of ribbons with hexagonally-packed pores (pore diameter of 8.6 nm). This folding creates microvoids in the particles that give rise to an additional porosity. The properties of adsorption/separation of this new type of silica were tested for HPLC. Although the powder was not optimized for this application, the first results on ungrafted silica appear equivalent to those obtained with a commercial HPLC silica powder. ***To cite this article: M.U. Martines et al., C. R. Chimie 8 (2005).***

Résumé

Nous décrivons la préparation d'un nouveau type de silice mésoporeuse de type MSU. Ce matériau a été préparé avec un coolymère trobloc de type Pluronic P123, selon le procédé de synthèse en deux étapes des silices MSU. Sa structure a été étudiée par diffraction des rayons X, mesures d'isothermes d'adsorption d'azote, microscopies électroniques à balayage et en transmission. L'étude par MET a été complétée par une étude de reconstruction tomographique tridimensionnelle, qui nous a permis d'obtenir une information détaillée sur la morphologie du système et son système poreux intraparticulaire. Cette poudre homogène est faite de nanoparticules de 200 nm formées par l'enroulement en pelote de rubans présentant une porosité structurale hexagonale (diamètre de pores de 8,6 nm). Cet enroulement crée une porosité additionnelle formée par des microcavités à l'intérieur des particules. Les propriétés d'adsorption et de séparation spécifiques de ce matériau, testées par chromatographie HPLC, ont permis d'élaborer des colonnes courtes potentiellement prometteuses pour de la chromatographie flash. ***Pour citer cet article : M.U. Martines et al., C. R. Chimie 8 (2005).***

* Corresponding author.
E-mail address: prouzet@iemm.univ-montp2.fr (E. Prouzet).
[1] Present address: Instituto Militar de Engenharia, Dept. de Engenharia Quimica (DE/5), Praça General Tiburcio 80, Praia Vermelha, CEP 22290-000 Rio de Janeiro, RJ, Brazil.
[2] Present address: 1, Carnation Close, East Malling, West Malling, ME 19 6EZ Kent, UK.

1631-0748/$ - see front matter © 2005 Académie des sciences. Published by Elsevier SAS. All rights reserved.
doi:10.1016/j.crci.2004.10.022

Keywords: Silica; Chromatography; Mesoporous; HPLC; Surfactant

Mots clés : Silice ; Chromatographie ; Mésoporeuse ; HPLC ; Tensioactifs

1. Introduction

The building of hierarchically organized porous compounds is one of the main goals in the present research on mesoporous materials. Many advantages are indeed expected from materials that could exhibit an organization at different scales both from the chemical and structural point of view [1]. If hierarchically ordered oxides were obtained by micropatterning of mesoporous oxides [2–5], one of the main objectives in this area is still to directly achieve a hierarchical porosity that would allow a facile access to the internal structure of the particles and increase the diffusion kinetics between the external medium and the internal surface. One possibility lies in synthesizing small mesoporous particles in order to combine the internal structural porosity of the materials with the external textural porosity between particles [6–12]. Another way consists of inducing a special design of the particles. In this domain, one may notice the very successful works of Lin et al. [13–17] who managed to synthesize successively "tubules-within-tubules" MCM-41, hollow spheres with an internal hierarchical order or pinholes, MCM-41 with a hollow tubular morphology or long rope morphology. Among the most original shapes, one may also notice the vesicle-like mesostructured silica (MSU-G) [18] and hollow helicoids [3]. However, basic methods to synthesize a mesoporous material with an accessible porosity are still good candidates and several works reported the successful preparation of mesoporous silica foam [8,19–22] or hollow particles [14,16,23–26].

We developed a proper method for the preparation of mesoporous silica with nonionic surfactants or block copolymers. This material, still named MSU-X because its first discovery by Pinnavaia's group at Michigan State University [27] (X =1, 2, 3, 4 depending on the nature of the template: alkyl, alkyl-aryl, copolymer or Tween, respectively), is defined, according to our process, by a two-step synthesis pathway implying the intermediate formation of silica-surfactant hybrid micelles [28–31]. Although block-copolymers have been used at first for the synthesis of MSU-3-type silica [27], the main development was relevant to Stucky's group at Santa Barbara UC, who reported the first synthesis of hexagonal mesoporous silica in acidic media, with large pores [32,33]. We reported that hexagonal stick-like particles of mesoporous silica prepared with Pluronic P123, could also be obtained with the two-step synthesis of MSU-X, in mild acidity and with the help of fluorine as condensation catalyst [29]. We present in this report a new type of silica developed with our two-step process and Pluronic P123 copolymer as template. One may point out that the present synthesis range in the same domain than those previously reported [29]. There are only "slight" changes in the process that regard the temperature of synthesis, relative concentrations in reagents and templates and pH. These variations are important because we used the Pluronic P123 block-copolymer as template [34]. This preparation was achieved thanks to a fine adjustment of the synthesis parameters, once the hybrid micelles had been obtained. We managed to prepare a new type of MSU-3 silica that exhibit a hierarchical structure made of nanoparticles (200 nm in size) that present folded ribbons of silica with regular large pores (8–9 nm in diameter), that entrapped large cavities inside the particles. This new morphology offers an easy access at three levels: small size of particles, large cavities inside the particles and a regular network of large pores. Its potential is illustrated by the first results in High Pressure Liquid Chromatography where a non-optimized short column filled with ungrafted silica exhibits promising separation properties.

2. Experimental

MSU-3 hexagonal mesoporous silica was prepared according to the two-step reaction process, already described, by using nonionic triblock copolymer surfactant as organic structure-directing agent. All reagents including the assembly agent–triblock copolymer Pluronic P123 ($EO_{20}PO_{70}EO_{20}$) from Aldrich Chemicals, the tetraethoxysilane (TEOS) silica source ($Si(OCH_2CH_3)_4$) from Fluka,, concentrated hydrochloric acid (SDS Co.) and sodium fluoride (Fluka Co.) were used as received. In a typical synthesis, 0.75 g (1.29 ×

10^{-3} mol) of Pluronic P123 was dissolved in 100 ml of deionized water previously acidified at pH 4 with concentrated hydrochloric acid (SDS Co.). After full dissolution, 3.33 g (0.016 mol) of TEOS was added at room temperature under moderate magnetic stirring. The solution, initially cloudy upon the TEOS addition, became quickly colorless, due to the hydrolysis of TEOS and the formation of the hybrid micelles [30]. After aging for 12 h at room temperature without stirring, this solution was heated to 45 °C in a thermostated shaking bath. The final condensation step was induced by the addition of 2.66 ml of sodium fluoride (0.25 M) (NaF/TEOS mol. ratio =4%) to the solution that was kept in the thermostated bath at 45 °C for 3 days, with slow shaking (40 rpm). The final product was filtered off and washed with water, air-dried at 100 °C, and calcined in air at 620 °C for 6 h with a 6 h preliminary step at 200 °C (heating rate of 3 °C/min).

SEM micrographs were obtained on a Hitachi S-5400 FEG microscope operating at 5 kV. The samples were covered with gold to increase conductivity. The X-ray diffraction patterns were acquired in transmission mode with 1 mm Lindemann capillaries. The X-ray diffractometer was a laboratory SAXS apparatus equipped with a copper rotating anode X-ray source ($\lambda \approx 1.54$ Å) (functioning at 4 kW) and with a multilayer focusing 'osmic' monochromator giving high flux (10^8 photons/s) and punctual collimation. An 'Image Plate' 2D detector was used. Diffraction patterns are reported as a function of the wave vector $q = 4\pi\sin\theta/\lambda$. For crystalline solids, the characteristic distance d_{hkl} between reticular plans hkl can be evaluated from the position of corresponding Bragg peak observed on the diffraction curve. Nitrogen adsorption isotherms were measured at 77 K on a Micromeritics 2010 sorptometer using standard continuous procedures, and samples were first degassed at 150 °C for 15 h. Surface area were determined by BET method in the 0.05–0.2 relative pressure range and pore diameter distribution by a polynomial relationship expanded from the Broekhoff and Boer (BdB) pore size distribution [7,35]. TEM was performed using a Philips CM30 T electron microscope with a LaB_6 filament as a source of electrons operated at 300 kV. Samples were mounted on Quantifoil® microgrid carbon polymer supported on a copper grid by placing a few droplets of a suspension of ground sample in ethanol on the grid, followed by drying at ambient conditions. All analyses refer to calcined materials.

For the 3D TEM Tomographic data acquisition, single axis tilt-series for TEM tomography were acquired automatically on a FEI Tecnai Sphera (T20 Twin) using the FEI XPlore3D Tomography Suite. The microscope was operated in TEM mode with parallel illumination; a large objective aperture was used to minimize the influence of diffraction effects and the defocus was set to –2 μm. The TEM projections were acquired on a bottom-mounted slow scan CCD camera with 1024 ×1024 pixels (Gatan 794). Seventy-one electron micrographs were collected over an angular range of ±70° in 2° steps. Re-centering and re-focusing of the area of interest after tilting were done automatically by combining precalibration of the goniometer movements with active shift and focus measurements as implemented in the XPlore3D acquisition software [36]. The active focus measurement was performed every three tilt-increments using the beam-tilt induced image shift and the active shift correction was done by acquiring additional tracking images every five tilt-increments [37]. The total acquisition time such a TEM tomography tilt-series is approximately 45 min. The tilt-series data were treated for image processing and reconstruction using IMOD Version 2.66 developed for 3-dimensional electron microscopy of cells at the Boulder Laboratory by David Mastronarde, James Kremer, and Rick Gaudette. Before tomographic reconstruction, the tilt-series has to be aligned precisely with respect to a common tilt-axis, thereby minimizing both blurring of small features and artifacts in the reconstruction. In IMOD this is achieved by a combination of rough cross-correlation alignment and least-square fitting of fiducial markers such as gold nano particles. Fourteen markers (well distributed over the imaged area) were tracked throughout the tilt-series and were used as the basis to refine *x*–*y* image shifts, average tilt-axis rotation, tilt-angle and magnification. The residual error for the marker tracking was 0.7 pixels. Following the image alignment, the 3D volume was reconstructed using weighted back-projection. A virtual slice of a particle was reconstructed from this 3D building.

The powder for HPLC tests was prepared as follows: 10 g of the calcined powder was dispersed in 250 cm^3 of water and the suspension was maintained by magnetic stirring. A 360 W (effective transmitted power of 150 W) US pulses (1 s on, 1 s off) was then applied three times for 10 min each to break the aggre-

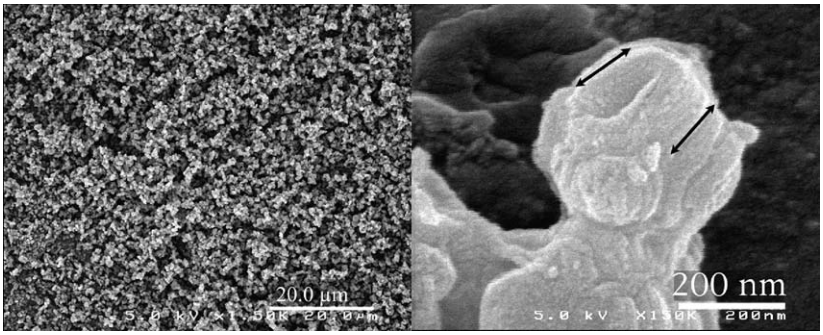

Fig. 1. SEM observation of the calcined MSU-3 silica powder.

gates. The tests were carried out with a liquid chromatograph equipped with a Waters pump (M501), a manual U6K injector (Waters), a UV visible variable wavelength detector (Dionex) and a Varian 4400 integrator. 10 µl of a 20–60 ppm test solution (benzene, naphthalene, phenantrene) was injected for chromatographic separation, the eluent flow being set at 1 ml/min. The eluent phase was composed of pure n-hexane. Silica columns (4 mm inner diameter) were homemade by filling the column with a cyclohexane slurry injection (under 300 bar nitrogen pressure).

3. Results and discussion

The observation of the calcined powder confirms that all the batch is very homogeneous and made of submicronic particles (Fig. 1a). A closer observation of a single particle reveals a mean particle size of about 200 nm (Fig. 1b). These particles do not exhibit any hexagonal shape but some preferential growth direction is observed (see arrow). The X-ray diffraction pattern of this sample exhibits three lines corresponding to the 100, 110 and 200 planes of the hexagonal *P6mm* space group, respectively (Fig. 2). This structure is similar to that reported for MCM-41 and SBA-15, with a cell parameter $a = 2\ d_{100}/\sqrt{3} = 121$ Å ($d_{100} = 104.7$ Å). Unlike MCM-41, SBA-15 and even our previous syntheses of hexagonal silica, there is no obvious relationship between the nanostructure of the silica framework and the morphology of the particles. The pore size distribution was determined by the adsorption/desorption isotherms of nitrogen. First, we compared this isotherm with that of hexagonal rod-like particles of MSU-3 silica previously reported (see inset in Fig. 3a) [29]. For the new material, the isotherm presents a steep adsorption jump at $P/P_o = 0.7$ corresponding to a narrow pore diameter distribution of 8.6 nm (see inset) (specific surface area ≈600 m^2/g). The desorption curve exhibits a small hysteresis as expected for these relative pressures, characteristic of well-defined pores with no restriction. One may notice also a vertical shift of the desorption curve, between $P/P_o = 0.45$ and 0.6. A convincing explanation for such a phenomenon was provided by Van der Voort et al., who reported that the plugging of mesopores by internal silica nanocapsules or metallic nanoparticles, could give this two-step desorption branch [38–40]. Even though we did not yet identify any similar blocking of the silica pores, we may assume the possible presence of microporous silica inside some pores. From these results, one may point

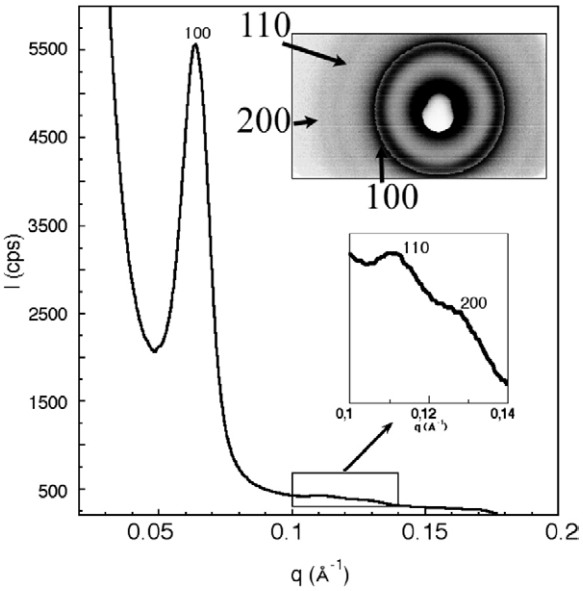

Fig. 2. Small-angle X-ray diffraction pattern of the calcined MSU-3 silica powder (inset: image plate pattern).

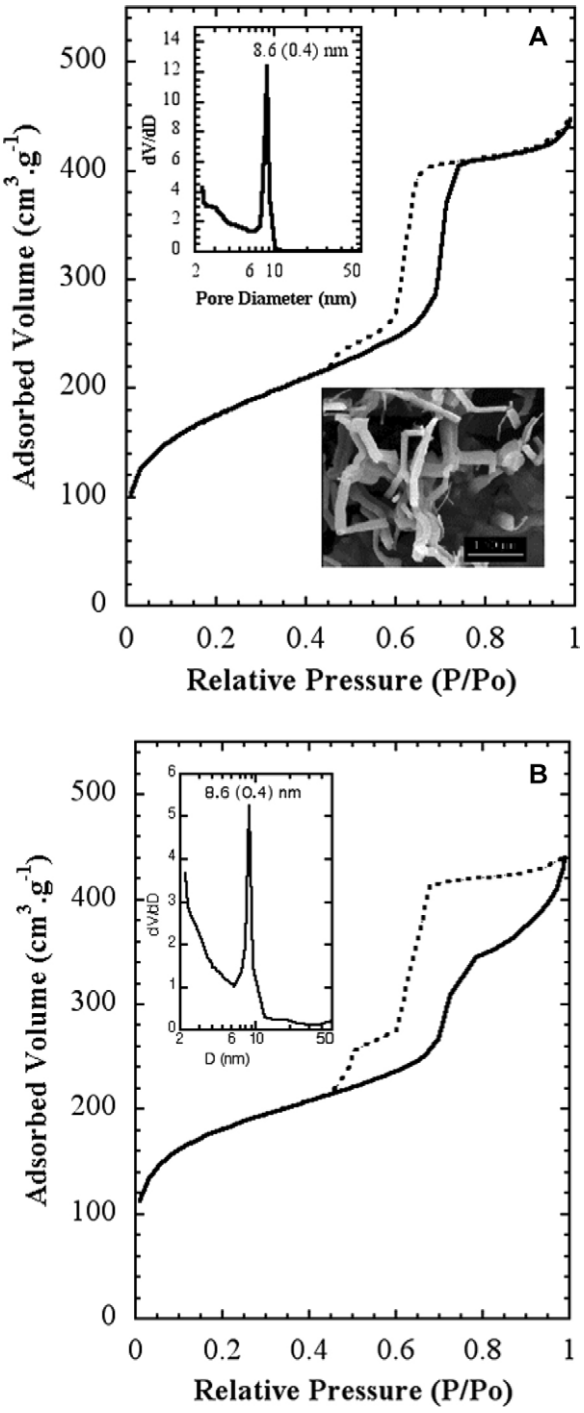

Fig. 3. Nitrogen adsorption/desorption isotherms of calcined MSU-3 silica: (a) stick-like particles ([23]); (b) the present study.

out the main differences observed for the silica reported in the present study. Actually, it displays almost the same features as observed for rod-like particles, especially the same pore size and the desorption plateau below $P/P_o = 0.6$, but some additional features are observed too (Fig. 3b): there is a more progressive step in the adsorption branch and the hysteresis is sharper.

We performed TEM studies in order to solve the structure of these particles. The observation of a single particle (Fig. 4) reveals that some areas in the particle exhibit parallel pores stacked as a honeycomb, but images such at these, hardly help to build a complete model. We overcame this problem by performing a 3D TEM tomography analysis that allowed us to reconstruct the internal structure of the particle. First, a full set of pictures was taken on a single particles, with different tiltings. Examples of photos are given in Fig. 5 where honeycomb structures can be identified (the black dots are gold nanoparticles deposited for the position calibration). Virtual slices of this particle could be calculated from this set of photos (Fig. 6). The fine structure of this material appears as if made with a folded ribbon of hexagonally packed mesoporous silica. This folding creates cavities inside the particle, which must give rise to the additional features observed in the nitrogen isotherms. Hence, three factors may increase the future diffusion and reaction of species in this material: the small size, the cavities and the structural large porosity.

The effect of this new microstructure was tested in HPLC separation with ungrafted powders. Since almost their discovery, mesoporous silica were assumed to be good candidates for this application because they

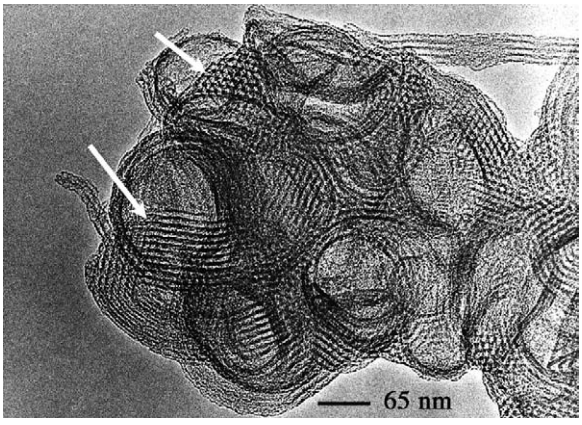

Fig. 4. TEM observation of the calcined MSU-3 silica powder.

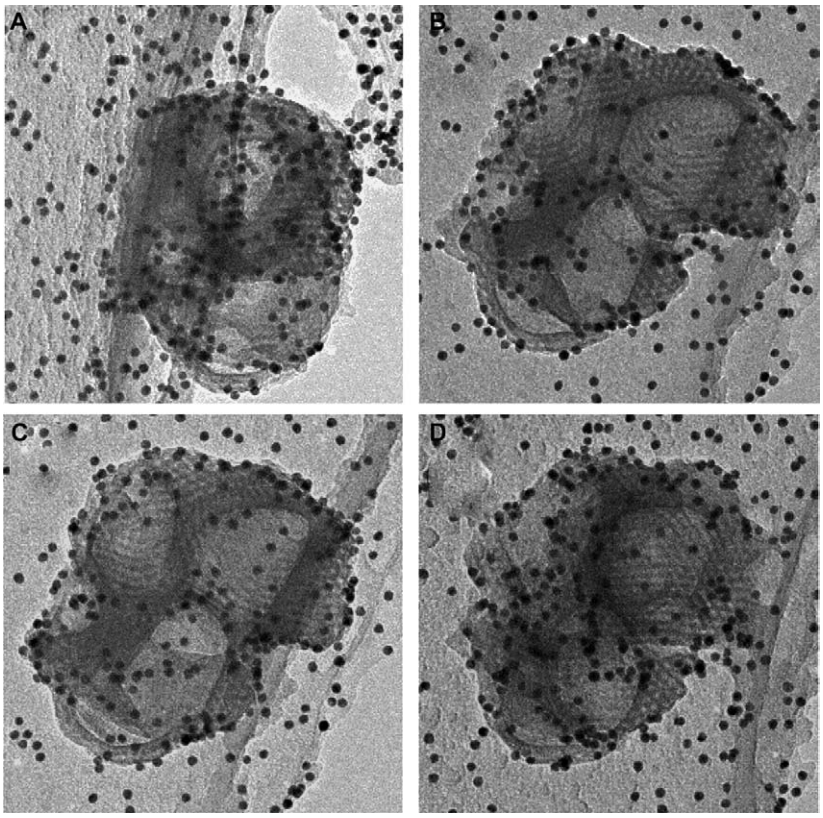

Fig. 5. TEM photos of the same particle with different tiltings. These photos were used for the 3D rebuilding of the internal structure of the calcined MSU-3 silica powder.

exhibit high surface area and a well-defined porosity [11,41,42]. Large pores mesoporous silica of the SBA-15 type, prepared with Pluronic P123 in acidic pH was tested also, but mostly for biomolecules separation based on size exclusion [43,44]. From our knowledge, the only test that was performed on reverse chromatog-

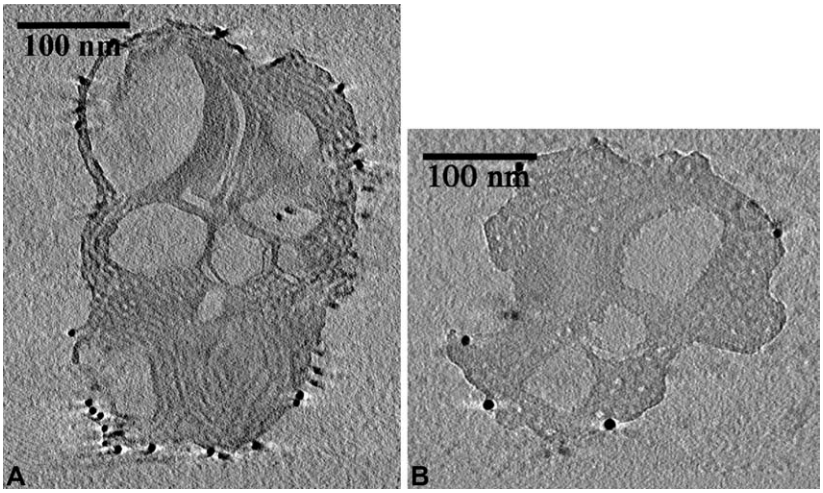

Fig. 6. Internal structure of the calcined MSU-3 silica powder rebuilt from TEM 3D tomography.

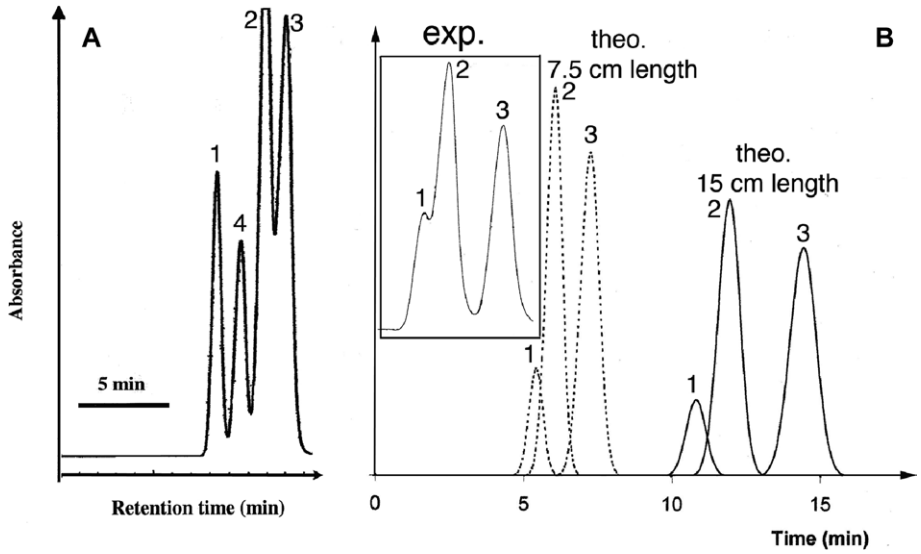

Fig. 7. HPLC separation tests performed with benzene (1), naphthalene (2), phenantrene (3) and biphenyl (4) for: (a) a commercial powder with a column length of 25 cm; (b) the present MSU-3 powder with a column length of 6.25 cm along with theoretical chromatograms calculated for different lengths.

raphy with grafted micrometric spherical SBA-15 silica, exhibited rather asymmetric peaks with a quite broad tail, compared with commercial powders [45]. In usual applications, powders required for HPLC, must exhibit a particle size bigger than 2 μm in order to limit the pressure required for 'pushing' the eluent and the HPLC columns have generally a length of 20–30 cm. This goal is better achieved if one manages to synthesize spherical particles with a monodisperse size distribution [45–47]. However, these configurations may be highly consuming in products and parallel methods have been explored in order to increase sensibility, efficiency and decrease the consumption. To this purpose, high-resolution as well as electrokinetic separations were developed [46,48–50].

Our pristine particles exhibit sizes close to 200 nm, which is a priori incompatible with HPLC applications because they would imply a too high pressure. One might shorten this column if one desires to decrease the pressure, but this would imply a lower retention efficiency. This drawback can be overcome only if the powder exhibits a higher specific surface area and/or adsorption capacity. Finally, one of the main parameters to achieve an efficient column is the quality of the particle packing, which implies a narrow distribution of the particle size. This latter characteristic is usually achieved by a drastic selection in particle size. We demonstrated previously that MSU-type mesoporous silica could be used for HPLC separation and that they exhibit good adsorption properties [47]. Since we could expect a higher interaction with the present material, we explored the possibility to build short columns of 6 cm length. We display for comparison the separation results that were obtained with a 25-cm-length column of a commercial powder (Nucleosil 7–50) (benzene, biphenyl, naphthalene and phenantrene) (Fig. 7a) [47]. It is compared with that of a 6.25 cm length column filled with our MSU-3 powder (benzene, naphthalene and phenantrene) (Fig. 7b, exp). This latter was only de-aggregated by ultrasound and we did not use any operation of size selection. This experiment was completed by simulation of chromatograms to probe the column efficiency as a function of the column length. The separation of benzene, naphthalene and phenantrene is achieved, even with this short length and the peaks remain symmetric. Hence, the structure of this new type of mesoporous silica, combined with its special topology allowed us to overcome the drawbacks imposed by the small particle size by decreasing the column length down to 6.25 cm and still obtaining a good separation (see Fig. 7b exp.). We observe that the results obtained with this powder that was not optimized, are quite similar to those obtained with a commercial powder.

References

[1] C. Sanchez, G.J.D. Soler-Illia, F. Ribot, D. Grosso, C.R. Chimie 6 (2003) 1131.

[2] P. Yang, T. Deng, D. Zhao, P. Feng, D.J. Pine, B.F. Chmelka, G.M. Whitesides, Science 282 (1998) 2244.

[3] S.M. Yang, I. Sokolov, N. Coombs, C.T. Kresge, G.A. Ozin, Adv. Mater. 11 (1999) 1427.

[4] P. Yang, A.H. Rizvi, B. Messer, B.F. Chmelka, G.M. Whitesides, G.D. Stucky, Adv. Mater. 13 (2001) 427.

[5] Z.Y. Yuan, A. Vantomme, A. Léonard, B.-L. Su, J. Chem. Soc., Chem. Commun. (2003) 1558.

[6] P. Tanev, T.J. Pinnavaia, Science 267 (1995) 865.

[7] E. Prouzet, F. Cot, G. Nabias, A. Larbot, P.J. Kooyman, T.J. Pinnavaia, Chem. Mater. 11 (1999) 1498.

[8] L. Huerta, C. Guillem, J. Latorre, A. Beltran, D. Beltran, P. Amoros, J. Chem. Soc., Chem. Commun. (2003) 1448.

[9] A. Lind, C. Du Fresne von Hohenesche, J.-H. Smatt, M. Linden, K.K. Unger, Micropor. Mesopor. Mater. 66 (2003) 219.

[10] G. Büchel, K.K. Unger, A. Matsumoto, K. Tsutsumi, Adv. Mater. 10 (1998) 1036.

[11] G. Büchel, M. Grün, K.K. Unger, A. Matsumoto, K. Tsutsumi, Supramol. Sci. 5 (1998) 253.

[12] L. Mercier, T.J. Pinnavaia, Adv. Mater. 9 (1997) 500.

[13] H.-P. Lin, C.-Y. Mou, Science 273 (1996) 765.

[14] H.-P. Lin, Y.-R. Cheng, C.-Y. Mou, Chem. Mater. 10 (1998) 3772.

[15] H.-P. Lin, S.-B. Liu, C.-Y. Mou, C.-Y. Tang, J. Chem. Soc., Chem. Commun. (1999) 583.

[16] H.-P. Lin, S. Cheng, C.-Y. Mou, Chem. Mater. 10 (1998) 581.

[17] H.-P. Lin, C.-Y. Mou, S.-B. Liu, C.-Y. Tang, J. Chem. Soc., Chem. Commun. (2001) 1970.

[18] S.-S. Kim, W. Zhang, T.J. Pinnavaia, Science 282 (1998) 1302.

[19] S.A. Bagshaw, J. Chem. Soc., Chem. Commun. (1999) 767.

[20] P. Schmidt-Winkel, W.W.J. Lukens, D. Zhao, P. Yang, B.F. Chmelka, G.D. Stucky, J. Am. Chem. Soc. 121 (1999) 254.

[21] P. Schmidt-Winkel, C.J. Glinka, G.D. Stucky, Langmuir 16 (2000) 356.

[22] P. Schmidt-Winkel, W.W.J. Lukens, P. Yang, D.I. Margolese, J.S. Lettow, J.Y. Ying, G.D. Stucky, Chem. Mater. 12 (2000) 686.

[23] P. Bruinsma, A.Y. Kim, J. Liu, S. Bashkaran, Chem. Mater. 9 (1997) 2507.

[24] Z. Lei, J. Li, Y. Ke, Y. Zhang, H. Zhang, F. Li, X. Linyun, J. Mater. Chem. 11 (2001) 2930.

[25] E. Prouzet, F. Cot, C. Boissière, P.J. Kooyman, A. Larbot, J. Mater. Chem. 12 (2002) 1553.

[26] C. Yu, B. Tian, J. Fan, G.D. Stucky, D. Zhao, Chem. Lett. (2002) 62.

[27] S.A. Bagshaw, E. Prouzet, T.J. Pinnavaia, Science 269 (1995) 1242.

[28] C. Boissière, A. Van der Lee, A. El Mansouri, A. Larbot, E. Prouzet, J. Chem. Soc. Chem. Commun. 20 (1999) 2047.

[29] C. Boissière, A. Larbot, A. Van der Lee, P.J. Kooyman, E. Prouzet, Chem. Mater. 12 (2000) 2902.

[30] C. Boissière, A. Larbot, C. Bourgaux, E. Prouzet, C.A. Bunton, Chem. Mater. 13 (2001) 3580.

[31] C. Boissière, M.A.U. Martines, M. Tokomuto, A. Larbot, E. Prouzet, Chem. Mater. 15 (2003) 509.

[32] D. Zhao, J. Feng, Q. Huo, N. Melosh, G.H. Fredrickson, B.F. Chmelka, G.D. Stucky, Science 279 (1998) 548.

[33] D. Zhao, Q. Huo, J. Feng, B.F. Chmelka, G.D. Stucky, J. Am. Chem. Soc. 120 (1998) 6024.

[34] M.A.U. Martines, E. Yeong, A. Larbot, E. Prouzet, Micropor. Mesopor. Mater. 74 (2004) 213.

[35] J.C.P. Broekhoff, J.H. de Boer, J. Catal. 10 (1968) 377.

[36] U. Ziese, A.H. Janssen, J.L. Murk, W.J.C. Geerts, T. Krift, A.J. Verkleij, A.J. Koster, J. Microsc. 205 (2002) 187.

[37] A.J. Koster, A. Van den Bos, K.D. Van der Mast, Ultramicroscopy 21 (1987) 209.

[38] P. Van der Voort, P.I. Ravikovitch, K.P. de Jong, A.V. Neimark, A.H. Janssen, M. Benjelloun, E. Van Bavel, P. Cool, B.M. Weckhuysen, E.F. Vansant, J. Chem. Soc., Chem. Commun. (2002) 1010.

[39] P. Van der Voort, P.I. Ravikovitch, K.P. De Jong, M. Benjelloun, E. Van Bavel, A.H. Janssen, M. Benjelloun, E. Van Bavel, P. Cool, B.M. Wechuysen, E.F. Vansant, J. Phys. Chem. B 106 (2002) 5873.

[40] A.H. Janssen, C.-M. Yang, Y. Wang, F. Schüth, A.J. Koster, K.P. de Jong, J. Phys. Chem. B 107 (2003) 10552.

[41] D. Kumar, K. Schumacher, C. Du Fresne von Hohenesche, M. Grün, K.K. Unger, Colloids Surf. A 109 (2001) 187–188.

[42] T. Nassivera, A.G. Eklund, C.C. Landry, J. Chromatogr. A 973 (2002) 97.

[43] J. Zhao, F. Gao, Y. Fu, W. Jin, P. Yang, D. Zhao, J. Chem. Soc., Chem. Commun. 7 (2002) 752.

[44] A.L. Doadrio, E.M.B. Sousa, J.C. Doadrio, J. Perez Pariente, I. Izquierdo-Barba, M. Vallet-Regi, J. Control. Release 97 (2004) 125.

[45] M. Mesa, L. Sierra, B. Lopez, A. Ramirez, J.-L. Guth, Solid-State Sci. 5 (2003) 1303.

[46] K.K. Unger, D. Kumar, M. Odin, O. Buchel, S. Ludtke, T. Adam, K. Schumacher, S. Renker, J. Chromatogr. A 892 (2000) 47.

[47] C. Boissière, M. Kümmel, M. Persin, A. Larbot, E. Prouzet, Adv. Funct. Mater. 11 (2001) 129.

[48] S. Luedtke, T. Adam, N. Von Doehren, K.K. Unger, J. Chromatogr. A 887 (2000) 339.

[49] T. Adam, K.K. Unger, M.M. Dittmann, G.P. Rozing, J. Chromatogr. A 887 (2000) 327.

[50] M.L. Huber, T.P. Hennessy, D. Lubda, K.K. Unger, J. Chromatogr. B 803 (2004) 137.